Am J Cancer Res 2025;15(6):2826-2842
www.ajcr.us /ISSN:2156-6976/ajcr0164214

Original Article

Splicing factor 3b subunit 4 (SF3b4) is mediated by EP300 and CREBBP to promote colorectal cancer (CRC) proliferation by enhancing autophagy

Tianhao Wu, Zhongxiang Xiao, Bowen Su, Zaihua Yan, Yv Zhao, Cheng Huang, Lu Zhou, Hongpeng Tian, Guangjun Zhang

Department of Gastrointestinal Surgery, Affiliated Hospital of North Sichuan Medical College/Institute of Hepatobiliary Pancreatic and Intestinal Disease, North Sichuan Medical College, Nanchong, Sichuan, China

Received February 27, 2025; Accepted June 18, 2025; Epub June 25, 2025; Published June 30, 2025

Abstract: Splicing factor 3b subunit 4 (SF3b4) is closely associated with cancer development. As a core subunit of the SF3b complex, SF3b4 participates in regulating alternative splicing, and its abnormal expression is linked to the onset of malignant tumors. However, the role of SF3b4 in colorectal cancer (CRC) remains undefined. This study demonstrates that in CRC, E1A binding protein p300 (EP300) and CREB binding protein (CREBBP) regulate SF3b4 expression by activating Histone H3 lysine 27 acetylation (H3K27ac) on the SF3b4 promoter. Additionally, enhanced autophagy counteracts the proliferation-inhibitory effect of SF3b4 knockdown in CRC cells. Implications Statement: SF3b4 may promote CRC proliferation by enhancing cellular autophagy. SF3b4 acts as a potential oncogene in CRC tumorigenesis and progression. SF3b4 serves as a promising prognostic biomarker for CRC.

Keywords: Colorectal cancer, EP300, CREBBP, H3K27ac, SF3b4, proliferation, autophagy

Introduction

Colorectal cancer (CRC) is one of the most common malignant tumors with a high global incidence. According to the 2022 Global Cancer Statistics Report, CRC was the third most common malignant tumor worldwide (accounting for 9.6% of all malignancies) and the second most lethal cancer (accounting for 9.3% of all malignancies) in 2022, with an estimated 1.9 million new cases and 904,000 deaths [1]. Current primary treatments for CRC include surgery, chemotherapy, and targeted therapy, with immunotherapy also applied clinically. However, CRC is often diagnosed at advanced stage and develops resistance to chemotherapy and targeted therapy [2], leading to poor prognosis for patients. There is an urgent need to identify new and effective molecular targets to improve the prognosis of CRC patients.

Alternative splicing (AS) refers to the process by which precursor mRNA (pre-mRNA) generates different splicing variants through splicing during gene transcription. This process allows a single gene to encode multiple protein products, increasing the diversity of gene functions. Alternative splicing may play a role in cancer development and progression [3, 4]. Pre-mRNA splicing occurs in a large RNA-protein complex called the spliceosome, which is dynamically composed of small nuclear ribonucleoproteins (snRNPs) and protein factors. As a ribonucleoprotein complex, the spliceosome identifies pre-mRNA and splicing sites and catalyzes splicing reactions. SnRNPs involved in splicing include U1, U2, U4, U5, and U6. The SF3b complex is a multi-protein complex that plays an important role in the accurate excision of non-coding sequences from pre-mRNA. As a component of U2 snRNP, SF3b participates in pre-mRNA splicing and 3'-end processing [3]. The SF3b complex consists of 7 subunits, which have different names in various species due to differences in methods used to characterize the complex. For clarity, researchers have named these 7 subunits as SF3b1, SF3b2,

https://doi.org/10.62347/AHXI2343

SF3b3, SF3b4, SF3b5, SF3b6, and SF3b7 respectively [4].

Splicing factor 3b subunit 4 (SF3b4), a core subunit of the SF3b complex, is encoded by a gene localized to chromosome 1q12-q21 and participates in regulating alternative splicing. Its abnormal expression is typically associated with abnormal cell growth and can lead to the development of malignant tumors [5]. While abnormal expression of SF3b4 is a key factor in Nager syndrome [5-7], growing evidence shows that SF3b4 is highly expressed in hepatocellular carcinoma, ovarian cancer, cervical cancer, non-small cell lung cancer, and clear cell renal cell carcinoma, promoting the development of these malignancies. Conversely, SF3b4 is lowly expressed and acts as a tumor suppressor in pancreatic cancer and breast cancer [8-13]. Currently, the role of SF3b4 in CRC remains undefined.

Autophagy is a process by which cells degrade and recycle their own components to maintain cellular homeostasis by eliminating unnecessary or dysfunctional organelles and proteins. Autophagy is induced by stress conditions such as nutrient or energy deprivation, hypoxia, and cellular damage [14]. In CRC development, autophagy exhibits a dual role: on one hand, it can significantly inhibit CRC cell proliferation and induce apoptosis; on the other hand, it provides additional energy for CRC cells, promoting their abnormal proliferation and reducing CRC responsiveness to various treatments [15].

Some studies have shown that SF3b3 is involved in the regulation of autophagy in Invasive Breast Carcinoma (IBC) [16]. This indicates that alternative splicing and the SF3b complex may participate in autophagy regulation in tumor cells. As a subunits of the SF3b complex, SF3b4 exerts oncogenic effects by regulating malignant tumor proliferation [13], invasion [9], metastasis [11], alternative splicing of tumor-related genes [17-19], and mRNA transport efficiency [13]. However, whether SF3b4 affects the occurrence and development of malignant tumors through autophagy remains to be studied.

This study aims to detect the expression level of SF3b4 in CRC tissues and cells and determine its prognostic value in CRC patients. Additionally, we investigated the effects of SF3b4 on CRC cell proliferation and autophagy, as well as the regulation of SF3b4 expression by EP300 and CREBBP through activating histone H3 lysine 27 acetylation (H3K27ac) on the SF3b4 promoter.

Materials and methods

Patient samples

The study protocol was approved by the Ethics Committee of the Affiliated Hospital of North Sichuan Medical College (Nanchong, China) [Approval No. 2024ER284-1]. From March 2017 to February 2018, colorectal cancer (CRC) tissues and adjacent non-tumorous tissue samples were obtained from 92 CRC patients who underwent surgical resection at the Affiliated Hospital of North Sichuan Medical College. Specimens were frozen immediately in liquid nitrogen and stored at -80°C after resection.

The inclusion criteria were as follows: 1. Patients newly diagnosed with CRC by pathological examination for the first time; 2. No distant tumor metastasis detected. The exclusion criteria were: 1. Patients with other malignant tumors, hematological diseases, severe complications, and/or immune system diseases; 2. Patients who received chemotherapy, radiotherapy, or other treatments before surgery; 3. Patients unwilling to participate in this study. Among the 92 samples, 8 cases were excluded from the study due to subsequent detection of liver or lung metastasis, and 84 cases were finally included. This study was approved by the Ethics Committee of the Affiliated Hospital of North Sichuan Medical College in accordance with its relevant regulations and complied with the Declaration of Helsinki.

Cell line and culture

CRC cells lines (HCT116, HCT15, SW480, SW620, and LoVo) were purchased from JENNIO Biological Technology, and FHC cells (human normal colonic epithelial cell line) were obtained from BLUEFBIO. The CRC cell lines were cultured in PRMI-1640 medium (Invitrogen; Thermo Fisher Scientific Co., Ltd.) supplemented with 10% fetal bovine serum (FBS) and 100 U/ml streptomycin/penicillin. FHC cells were cultured in DMEM medium (Invitrogen;

Thermo Fisher Scientific Co., Ltd.) supplemented with 10% fetal bovine serum and 100 U/ml streptomycin/penicillin. FHC cells were maintained in DMEM medium (Invitrogen; Thermo Fisher Scientific Inc.) containing 10% FBS and 100 U/ml streptomycin/penicillin. All cells were cultured in a humidified incubator at 37°C with 5% CO_2.

Cell transfection

The cDNA encoding the CDS of ATG7 was amplified by PCR using I-5™ 2×High-Fidelity Master Mix (TsingKe, China), and then subcloned into the BamHI and XhoI sites of the pcDNA3.1 vector (IBSBIO, China). The constructed plasmid was aliased as pcDNA3.1-ATG7. The plasmid was digested with FastDigest Green Buffer (10×) (Invitrogen; Thermo Fisher Scientific Co., Ltd.) at 37°C for 1 hour, followed by ligation of the plasmid and target fragment using a T4 DNA Ligase kit (TaKaRa, Japan) in a total volume of 10 μL. After mixing thoroughly, the reaction was incubated at 16°C overnight.

siRNAs for silencing EP300 (si-EP300#1, si-EP300#2), CREBBP (si-CREBBP#1, si-CREBBP#2), SF3b4 (si-SF3b4#1, si-SF3b4#2), and corresponding negative controls were purchased from RiboBio (Guangzhou, China). Transfection was performed using Lipofectamine® 3000 (Invitrogen; Thermo Fisher Scientific Inc.) to deliver plasmids or siRNAs into CRC cells. The sequences of si-EP300#1 and si-EP300#2 were 5'-CGACTTACCAGATGAATTA-3' and 5'-GCACAAATGTCTAGTTCTT-3', respectively. The sequences of si-CREBBP#1 and si-CREBBP#2 were 5'-CGACAUGACUGUCCUGUUUGC-3' and 5'-GGAUGAAUAUUAUCACUUAUU-3', respectively. The sequences of si-SF3b4#1 and si-SF3b4#2 were 5'-GGAUGAGAAGGUUAGUGAATT-3' and 5'-GCACCAAGGCUAUGGCUUUTT-3', respectively. Before transfection, 2×10^5 HCT15 or HCT116 cells were seeded into 6-well plates and cultured at 37°C until reaching 70%-80% confluence. All cells were incubated at 37°C with 5% CO_2 for 72 hours before subsequent experiments. Western blotting and RT-qPCR were used to confirm transfection success and detect transfection efficiency.

To construct CRC cells with stable knockdown of SF3b4, Shanghai Genechem Co., Ltd. designed lentiviral short - hairpin RNAs (sh-RNAs/sh) targeting SF3b4. The sh-RNA sequences were: sh-SF3b4 forward: 5'-CCGGGGATGAGAAGGTTAGTGAATTCAAGAGATTCACTAACCTTCTCATCCTTTTTTG-3', reverse: 5'-AATTCAAAAAAGGATGAGAAGGTTAGTGAATCTCTTGAATTCACTAACCTTCTCATCC-3'. Stable SF-3b4-knockdown CRC cell lines were established using the pPACKH1 HIV Lentivector Packaging Kit (System Biosciences, LLC) according to the manufacturer's instructions. After 24 hours, PEG-it Virus Precipitation Solution (System Biosciences) was added to the collected medium and incubated at 4°C for 12 hours to concentrate viruses. The virus-containing medium was centrifuged at 60,000 rpm for 1.5 hours at 4°C. Virus particles were resuspended in PBS, aliquoted, and stored at -80°C. HCT15 and HCT116 cells were transfected with Polybrene (8 μg/ml) for 72 hours. Fluorescence intensity was observed under an inverted fluorescence microscope after 72 hours. Stably transfected HCT15 and HCT116 cells were selected with medium containing puromycin (8 μg/ml) and maintained at 4 μg/ml puromycin. Transfection efficiency and success were verified by Western blotting and RT-qPCR.

Reverse Transcription Quantification (RT-qPCR)

Total RNA was extracted from CRC tissues and cell lines using Trizol (Invitrogen; Thermo Fisher Scientific Co., Ltd.). To detect the expression of SF3b4 mRNA and EP300 mRNA, reverse transcription was performed using PrimeScript™ RT Master Mix (TaKaRa, Japan). Subsequently, SYBR Premix Ex Taq (TaKaRa, Japan) was used for detection on an ABI 7500 Real-Time PCR System (Applied Biosystems, Thermo Fisher Scientific Inc.). Expression of EP300 mRNA, CREBBP mRNA, and SF3b4 mRNA was detected using TB Green Premix Ex Taq II (TaKaRa, Japan). The RT-qPCR thermal cycling conditions were as follows: 95°C for 10 minutes; followed by 30 cycles of 95°C for 30 seconds, 60°C for 30 seconds, and 72°C for 30 seconds; with a final extension at 72°C for 2 minutes. The primer sequences used for RT-qPCR were as follows:

For EP300: Forward 5'-CATAGCCCATAGGCGGGTTG-3', Reverse: 5'-GCAGTGTGCCAAACCAGATG-3'; For CREBBP: Forward 5'-GTGCTGGCTG-

AGACCCTAAC-3', Reverse: 5'-GGCTGTCCAAATGGACTTGT-3'; For SF3b4: Forward: 5'-AGTCAACACCCACATGCCAA-3', Reverse: 5'-CACCCGTATTGGCTTCCCAT-3'; For ATG7: Forward 5'-GGAAAAGAACCAGAAAGGAGG-3', Reverse: 5'-GCAGCAGACATTTGACAGACAC-3'; For GAPDH: Forward: 5'-TGACTTCAACAGCGACACCCA-3', Reverse: 5'-CACCCTGTTGCTGTAGCCAAA-3'.

Relative gene expression levels were calculated using the $2^{-\Delta\Delta Ct}$ method. GAPDH was used as the internal reference gene for normalizing mRNA expression levels. Each experiment was performed with three biological replicates.

Western blotting test

Total proteins were extracted from cells using high-efficiency RIPA tissue/cell lysis buffer (Solarbio, China) and protease/phosphatase inhibitors (Solarbio, China). The proteins were transferred to PVDF membrane using the One-Step PAGE Gel Fast Preparation Kit (Omni-Easy™), and then blocked with Protein Free Rapid Blocking Buffer (×1) at room temperature for 40 minutes in the dark. Subsequently, the blocked PVDF membrane were then incubated with the following primary antibodies at 4°C overnight in the dark: Anti-EP300 (1:500; AF0674; Affint), Anti-CREBBP (1:1,000; Proteintech), Anti-SF3b4 (1:2,000; 10482-1-AP; Proteintech), Anti-H3K27ac (1:500; HA-500046; HUABIO), P62 (1:5,000; 18420-1-AP; Proteintech), Anti-LC3I/II (1:1,000; 14600-1-AP; Proteintech), Anti-ATG7 (1:500; Proteintech), Anti-GAPDH (1:20,000; 10494-1-AP; Proteintech). After the incubation with primary antibodies, the membrane was incubated with HRP-conjugated secondary antibody (1:5,000; Proteintech) at room temperature in the dark for 1 hour. Protein bands were visualized using ECL reagents (Omni-ECL™). GAPDH was used as the internal reference. Each experiment was performed with three biological replicates.

Cell proliferation test

The proliferation ability of CRC cells was detected using colony formation assay and Cell Counting Kit-8 (CCK-8). For the CCK-8 assay, transfected and untransfected colorectal cancer cells (HCT15 and HCT116) in the logarithmic growth phase were selected as experimental subjects. A total of 3×10^3 cells per well were seeded into 96-well culture plates and incubated at 37°C for 0, 24, 48, 72, and 96 hours. Then, 10 μl of CCK-8 reagent (Beyotime, China) was added to each well containing CRC cells, followed by further incubation at 37°C with 5% CO_2 for 4 hours. After incubation, the optical density (OD) value of each well was measured at a wavelength of 450 nm using a microplate reader and recorded.

For the colony formation assay, 1×10^3 cells were seeded into 6-well plates and cultured for approximately 7 days (until visible cell colonies were formed). The colonies were first fixed with 4% paraformaldehyde at room temperature in the dark for 15 minutes, and then stained with 0.1% crystal violet at room temperature in the dark for 15 minutes. Cell colonies were counted using Image J software (version 1.73; National Institutes of Health). Each experiment was performed with three biological replicates.

Xenograft tumor experiment

Stably transfected and untransfected colon cancer cells HCT15 and HCT116 in the logarithmic growth phase were selected as experimental subjects. The cells were digested into single-cell suspensions with 0.25% trypsin and collected for later use. Ten female BALB/c nude mice (aged 1-2 months) were randomly divided into two groups (5 mice per group). The stably transfected and untransfected HCT15 or HCT116 cell suspensions in the logarithmic growth phase were taken, and 2×10^7 cells were inoculated into the supra - scapular region of the right forelimb of each nude mouse. Four weeks after injection, all mice were sacrificed by inhalation of CO_2 (air replacement rate, 10%-30% per minute). Tumors were excised, weighed, and measured (maximum tumor diameter < 2 cm).

All mice were housed in a standard specific-pathogen-free (SPF) environment, with free access to water and sterile food at 22-25°C under a 12:12 light/dark cycle, and the bedding was changed every two days. The animal supplier was Sibefu (Beijing) Biotechnology Co., Ltd. The animal experimental protocol was approved by the Ethics Committee for Laboratory Animals of North Sichuan Medical College (Nanchong, China) [Approval No.: NSMC Ethic Animal Review [2024] No. 067].

Transmission electron microscope analysis

Transfected and untransfected colorectal cancer cells (HCT116 and HCT15) were examined using standard transmission electron microscopy (TEM). The cells were fixed and embedded for TEM analysis. Samples were observed using a JEM-1400FLASH transmission electron microscope under conditions of 90 nm section thickness, 80 kV voltage, and 12,000× magnification to assess changes in autophagosome number. Each experiment was performed with three biological replicates.

Autophagy detection of CRC cell lines

This experiment evaluated changes in autophagic levels in CRC cells by examining the expression of cytosolic form of LC3 (LC3-I), phosphatidylethanolamine-conjugated form of LC3 (LC3-II), and sequestosome 1 (SQSTM1/P62). Microtubule-associated protein 1A/1B-light chain 3 (LC3), a key protein in autophagy, serves as a reliable autophagic marker. LC3 exists as an inactive cytosolic form (LC3-I) and is converted into an active autophagosome membrane-bound form (LC3-II) through proteolysis and lipidation during autophagy. Therefore, LC3-II indicates autophagosome formation. P62, a selective autophagic receptor protein, binds to ubiquitinated proteins and directs them to autophagosomes for degradation, establishing an inverse relationship between P62 protein expression and autophagic activity.

In this study, the stubRF-sensGFP-LC3 lentivirus (Shanghai GeneChem Co., Ltd.) was used to visualize changes in the number of autophagosomes and autolysosomes. Green fluorescent protein (GFP) is quenched in autophagosomes, so green puncta in images reflect autophagosomes, while red puncta represent autolysosomes. Thus, the yellow and red puncta in merged images denote autophagosomes and autolysosomes. The number of autophagosomes in CRC cells was observed under a confocal microscope in three random fields of view, and the average number of autophagic puncta per cell was calculated to represent autophagic levels. Each experiment was performed with three biological replicates.

Chromatin Immunoprecipitation (ChIP)

Transfected and untransfected colorectal cancer cell line HCT116 was used as the experimental subject. The ChIP assay was performed using the SimpleChIP® Plus Sonication Chromatin IP kit (#56383, Cell Signaling Technology, MA, USA). The cells were fixed with 3% formaldehyde, lysed, and sonicated to extract DNA fragments (Absin, Shanghai, China). Immunoprecipitation was carried out using Anti-H3K27ac, Anti-EP300, Anti-CREBBP, and Anti-IgG, along with sonicated supernatant. Reverse transcription quantitative PCR (RT-qPCR) with SF3b4 promoter-specific primers was used for purification analysis. Each experiment was performed with three biological replicates.

Bioinformatics analysis

The Cancer Genome Atlas (TCGA, https://www.cancer.gov/ccg/research/genome-sequencing/tcga) and UALCAN database (http://ualcan.path.uab.edu/) [20, 21] were used to validate SF3b4 expression in CRC and normal colorectal tissues. Immunohistochemical staining images of SF3b4 expression in CRC and normal colorectal tissues were obtained from the Human Protein Atlas (THPA, https://www.proteinatlas.org). To evaluate the impact of high vs. low SF3b4 expression on postoperative overall survival (OS) in CRC patients, Kaplan-Meier survival analysis curves were generated using the online bioinformatics tool Kaplan-Meier Plotter (https://kmplot.com/analysis/index.php?p=service&cancer=colon) [22, 23].

For investigating the mechanisms underlying SF3b4 overexpression in CRC, promoter modifications of SF3b4 were analyzed using the UCSC Genome Bioinformatics website (http://genome.ucsc.edu/) [24]. Gene expression correlations between EP300, CREBBP, and SF3b4 were assessed via GEPIA2 (http://gepia2.cancer-pku.cn/#index). Subsequently, SF3b4-associated gene data from the TCGA colorectal cancer (CRC) dataset were downloaded from the cBioPortal database (https://www.cbioportal.org/), followed by functional enrichment and pathway enrichment analyses using WebGestalt (https://www.webgestalt.org/).

Statistical methods

In this study, each experiment was independently repeated at least three times. The data in each group were indicated to follow normal distribution by homogeneity of variance test and are presented as mean ± standard deviation (Mean ± SD). Statistical analyses were conducted using SPSS 29.0.1.0 and Graphpad Prism 9.5.0. Statistical differences between two groups were determined by unpaired t-test, while differences between paired tumor and adjacent tissues were assessed by paired t-test. Categorical data were analyzed using chi-square test.

The Kaplan-Meier method was used to analyze the postoperative overall survival (OS) time of CRC patients, and log-rank test was applied to statistically compare survival rates between groups. Univariate and multivariate Cox proportional hazards models were used to evaluate SF3b4 as an independent prognostic factor for overall survival (OS). A P value < 0.05 was considered statistically significant.

Results

Expression level of SF3b4 in CRC tissues and cell lines

Expression levels of SF3b4 in CRC tissues and adjacent normal tissues were queried using the The Cancer Genome Atlas (TCGA) and UALCAN databases. Results showed that SF3b4 expression was significantly higher in CRC tissues than in adjacent normal tissues (**Figure 1A**, **1B**). Analysis of immunohistochemical image data from the Human Protein Atlas (THPA) database revealed high SF3b4 expression in CRC tissues (**Figure 1C**). Additionally, upregulated SF3b4 expression was observed in collected primary CRC tissues compared with adjacent normal tissues (**Figure 1D**). Western blotting and RT-qPCR showed that SF3b4 expression levels in CRC cell lines were significantly higher than those in the human normal colonic epithelial cell line FHC (**Figure 1E**). Western blotting also demonstrated that SF3b4 expression in CRC tissues was significantly higher than in paired adjacent normal tissues (n=8) (**Figure 1F**). Taken together, these results indicate that SF3b4 expression is significantly elevated in colorectal cancer tissues and cells compared with normal colorectal tissues and cells.

Relationship between SF3b4 expression and clinical and pathological features of CRC patients

To determine the association between SF3b4 expression and clinicopathological features, relative quantitative qPCR (2-ΔΔCt method) was used to measure SF3b4 mRNA expression. Based on the median expression value as the cutoff, 84 CRC patients were divided into high SF3b4 expression group (n=45) and low SF3b4 expression group (n=39). As shown in **Table 1**, high SF3b4 expression was correlated with lymph node metastasis, poor differentiation, and larger tumor size in CRC, suggesting that SF3b4 expression may be associated with CRC proliferation.

Survival curves were plotted according to patient survival status and follow-up time, revealing that CRC patients with high SF3b4 expression had shorter postoperative overall survival time. This result was further validated by Kaplan-Meier survival analysis using the online bioinformatics tool Kaplan-Meier Plotter (https://kmplot.com/analysis/index.php?p=service&cancer=colon) (**Figure 1G**).

As shown in **Table 2**, Cox proportional hazards regression models were used to identify factors influencing overall survival (OS) in CRC patients. Univariate Cox analysis showed that survival time was associated with T stage, lymph node metastasis, tumor differentiation, and SF3b4 expression. Additionally, multivariate Cox analysis indicated that T stage, lymph node metastasis, and SF3b4 expression were independent prognostic factors for OS in CRC patients. These findings suggest that SF3b4 may be involved in the development and progression of CRC and serve as an independent prognostic factor for CRC patients.

In CRC, EP300-mediated H3K27ac promotes SF3b4 expression

To investigate the regulatory mechanism of SF3b4 in CRC development, the UCSC Genome Bioinformatics website (http://genome.ucsc.edu/) was used to analyze SF3b4 promoter modifications (**Figure 2A**). Notably, significant enrichment of histone H3 lysine 27

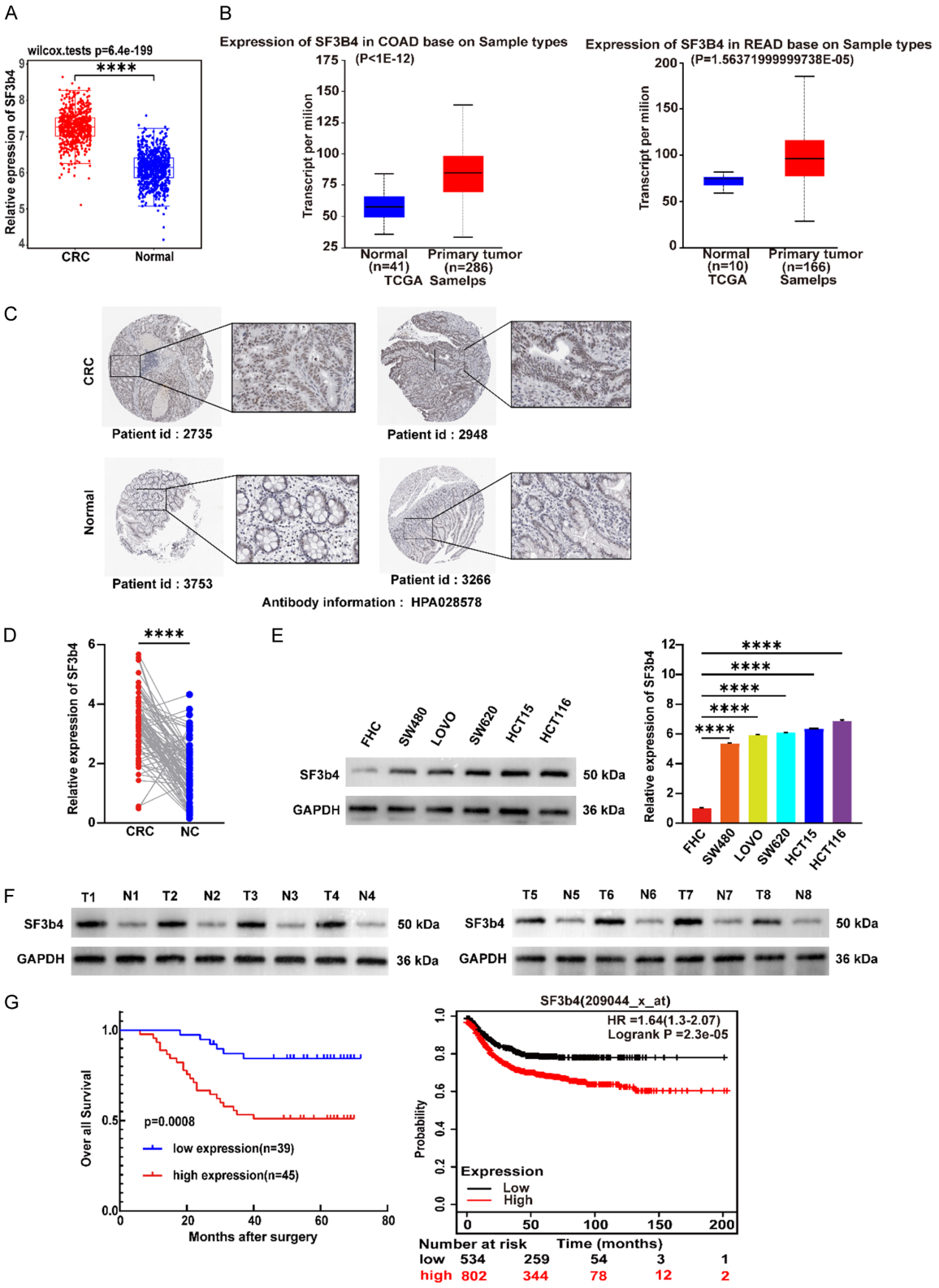

Figure 1. SF3b4 is upregulated in CRC tissues and cell lines compared with normal colorectal tissues and cells. A. SF3b4 expression in colorectal cancer was obtained from The Cancer Genome Atlas (TCGA) and statistically analyzed using R software v4.0.3. B. SF3b4 expression in colon and rectal cancer was obtained from the UALCAN database, with $^{*}P < 0.05$ considered statistically significant. C. Immunohistochemical staining of SF3b4 expression downloaded from The Human Protein Atlas database. D. Relative expression of SF3b4 in colorectal cancer and adja-

cent normal tissues determined by RT-qPCR. E. Protein levels of SF3b4 in normal colonic cell line FHC and colorectal cancer cell lines (LoVo, SW480, SW620, HCT116, and HCT15) measured by western blotting and RT-qPCR. F. Protein expression levels of SF3b4 in colorectal cancer tissues and paired adjacent normal tissues determined by western blotting (n=8). G. Kaplan-Meier survival analysis curves of postoperative overall survival time in CRC patients based on SF3b4 expression. OS Kaplan-Meier survival curves were plotted using the online bioinformatics tool Kaplan-Meier Plotter (https://kmplot.com/analysis/index.php?p=service&cancer=colon) ($^{*}P < 0.05$). Data are presented as the mean ± standard deviation (SD) of three independent experiments. Compared with the control group, $^{*}P < 0.05$, $^{****}P < 0.0001$.

Table 1. Correlation between SF3b4 expression and clinicopathological parameters in 84 colorectal cancer (CRC) patients (*P < 0.05)

Variable	SF3b4 expression		*P*-value
	High (n=45)	Low (n=39)	
Gender			0.816
Male	21	20	
Female	24	19	
Age			0.331
< 60	9	15	
≥ 60	36	24	
T stage			0.912
T1 and T2	26	23	
T3 and T4	19	16	
Lymph node metastasis			0.009*
Absent	16	14	
Present	29	25	
Differentiation			0.011*
Well	11	17	
Moderate	12	15	
Poor	22	7	
Tumor size			0.004*
< 5 cm	18	28	
≥ 5 cm	27	11	
Tumor Location			0.650
Colon	22	21	
Rectum	23	18	

*P < 0.05. SF3b4: splicing factor 3b, subunit 4.

acetylation (H3K27ac) signals was detected in the SF3b4 promoter region, suggesting that SF3b4 expression is regulated by histone acetylation. Previous studies have shown that H3K27ac can be regulated by EP300 and CREBBP [25]. HCT15 and HCT116 cells were treated with C646, a histone acetyltransferase inhibitor targeting EP300 and CREBBP. Western blotting revealed significantly reduced expression of H3K27ac and SF3b4 (**Figure 2B**).

Gene correlation analysis using GEPIA2 showed positive correlations between EP300 and SF3b4, as well as between CREBBP and SF3b4 ($P < 0.05$, $*R* > 0$) (**Figure 2C**). In HCT116 cells, specific siRNAs targeting EP300 were used for silencing. Western blotting and RT-qPCR confirmed successful transfection, showing decreased expression of H3K27ac and SF3b4 following EP300 knockdown (**Figure 2D**). Similarly, silencing CREBBP with specific siRNAs resulted in reduced H3K27ac and SF3b4 expression (**Figure 2E**). Chromatin immunoprecipitation (ChIP) assays further demonstrated that silencing EP300 or CREBBP decreased H3K27ac signal enrichment in the SF3b4 promoter (**Figure 2F**, **2G**). Co-silencing EP300 and CREBBP with siRNAs led to a more pronounced reduction in H3K27ac and SF3b4 expression compared to single knockdowns, consistent with results from C646-treated CRC cells (**Figure 2H**).

Collectively, these data indicate that EP300 and CREBBP activate H3K27ac acetylation on the SF3b4 promoter, upregulating its transcription and expression in CRC cells (**Figure 2I**).

Effects of SF3b4 on the proliferation of CRC cells

Next, we investigated the effect of SF3b4 expression on the proliferation of CRC cells. SF3b4 was silenced in HCT15 and HCT116 cells using si-RNAs. Verification by Western blotting and RT-PCR (**Figure 3A**, **3B**) showed that both si-RNA sequences effectively suppressed SF3b4 expression. The Cell Counting Kit-8 (CCK-8) and colony formation assays were used to assess the impact of SF3b4 on CRC cell proliferation capacity. Results showed that proliferation of SF3b4-silenced CRC cells was significantly reduced (**Figure 3C-E**).

Table 2. Univariate and multivariate cox proportional hazards regression analysis of postoperative overall survival in colorectal cancer patients (*P < 0.05)

Variable	Univariate analysis			Multivariate analysis		
	HR	95% CI	*P*-value	HR	95% *CI*	*P*-value
Gender	1.063	0.507-2.231	0.871			
Age	0.728	0.336-1.579	0.422			
T stage	2.954	1.361-6.415	0.006*	2.359	1.068-5.212	0.034*
Lymph node metastasis	9.318	2.208-39.319	0.002*	6.779	1.547-29.702	0.011*
Differentiation	1.671	1.041-2.680	0.033*	1.123	0.679-1.589	0.652
Tumor size	1.316	0.735-3.251	0.251			
Tumor location	0.880	0.419-1.849	0.736			
SF3b4 expression	4.114	1.666-10.160	0.002*	3.367	1.248-9.086	0.017*

*P < 0.05. HR: hazard ratio; CI: confidence interval; SF3b4: splicing factor 3b, subunit 4.

To further validate the effect of SF3b4 on CRC cell proliferation in vivo, stable SF3b4-knockdown HCT15 and HCT116 cell lines were established via lentiviral transfection and validated by Western blotting and RT-qPCR (**Figure 3F**, **3G**). BALB/c nude mice were then used to construct CRC xenograft models. Compared with the sh-Ctrl group, the sh-SF3b4 group exhibited significantly reduced weight and volume of xenograft tumors (**Figure 3H**, **3I**). These results indicate that reduced SF3b4 expression inhibits the proliferation capacity of CRC cells both in vitro and in vivo.

Effect of SF3b4 on CRC cell autophagy

To investigate whether SF3b4 expression affects autophagy in CRC cells, Western blotting was used to detect the expression of autophagic markers P62 and LC3I/II in xenograft tumors. Results showed that autophagic levels in xenograft tumors with stable SF3b4 knockdown were lower than those in the control group, with P62 expression higher and LC3I/II expression lower in the knockdown group (**Figure 4A**). This indicates that low SF3b4 expression reduces autophagic levels in vivo CRC cells.

For in vitro analysis of SF3b4's effect on autophagy, Western blotting was performed on control (sh-Ctrl) and SF3b4-knockdown (sh-SF3b4) CRC cells. Compared with the control group, SF3b4-knockdown cells exhibited upregulated P62 protein expression and significantly downregulated LC3I/II expression (**Figure 4B**), suggesting that low SF3b4 expression decreases autophagic levels in vitro.

Autophagy-related proteins (ATG proteins), including autophagy-related 7 (ATG7), a key autophagic effector enzyme [26], regulate critical stages of autophagy. To further clarify whether SF3b4 affects autophagosome formation in vitro, pcDNA3.1-ATG7 was transfected into sh-Ctrl and sh-SF3b4 cells to construct autophagy-enhanced groups (sh-Ctrl+pcDNA3.1-ATG7 and sh-SF3b4+pcDNA3.1-ATG7). This experiment aimed to validate whether autophagy regulates CRC cell proliferation and whether SF3b4 influences proliferation by modulating autophagy. Western blotting showed that compared with sh-Ctrl, sh-Ctrl+pcDNA3.1-ATG7 exhibited decreased P62 and increased LC3I/II expression. Similarly, sh-SF3b4+pcDNA3.1-ATG7 showed reduced P62 and elevated LC3I/II compared with sh-SF3b4 (**Figure 4C**).

Ultrastructural analysis via transmission electron microscopy (TEM) revealed changes in autophagosome numbers across groups (**Figure 4D**, **4E**). Laser confocal microscopy using stubRFP-sensGFP-LC3 lentiviral labeling further visualized autophagosome and autolysosome dynamics (**Figure 4F**, **4G**). In vitro, sh-SF3b4 cells showed significantly fewer autophagosomes than sh-Ctrl, while autophagy-enhanced sh-Ctrl+pcDNA3.1-ATG7 cells had increased autophagosomes. Notably, sh-SF3b4+pcDNA3.1-ATG7 cells also exhibited more autophagosomes than sh-SF3b4, indicating that ATG7 overexpression reverses SF3b4-knockdown-induced autophagic inhibition.

CCK-8 and colony formation assays further showed that autophagy enhancement via ATG7

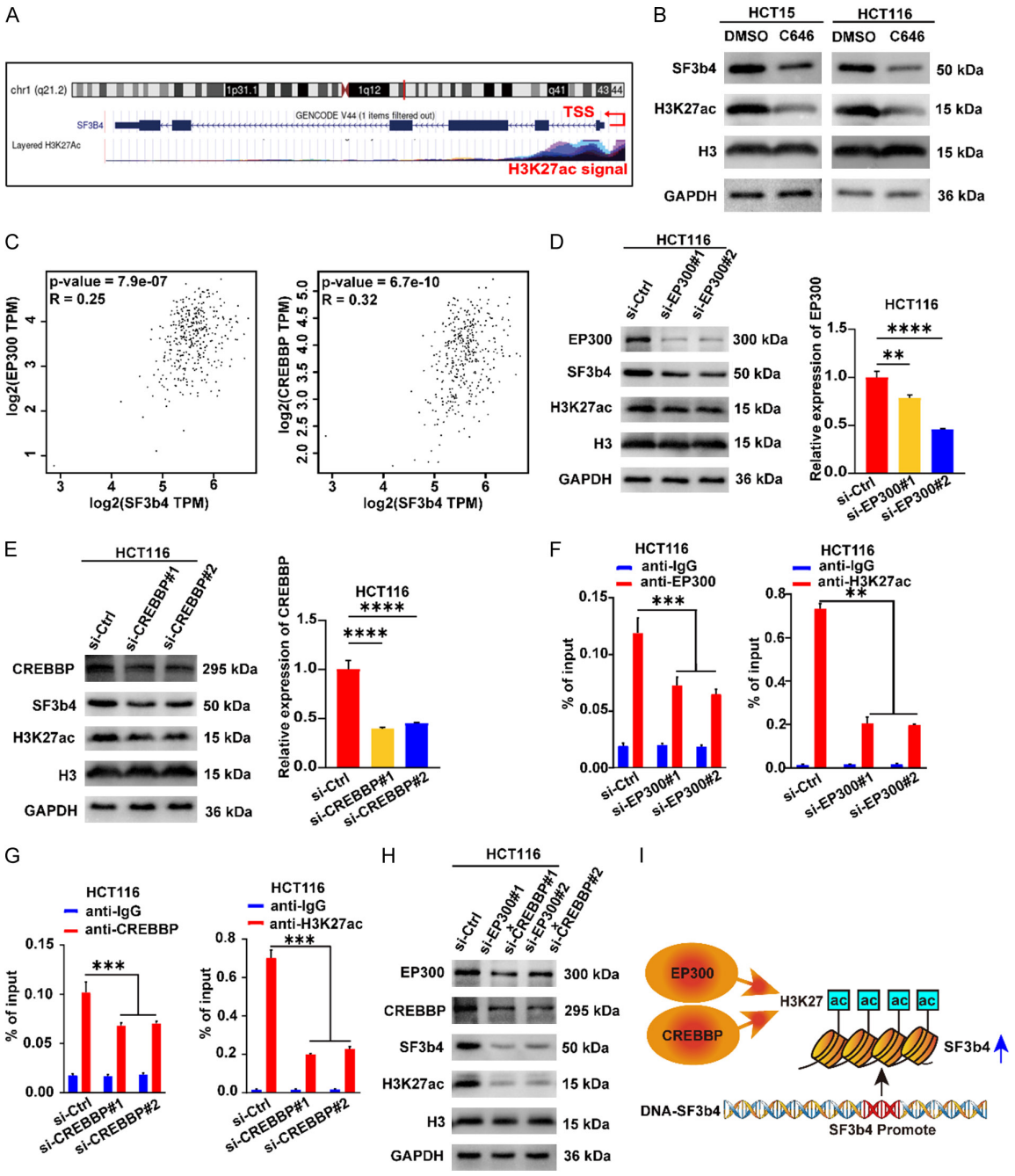

Figure 2. EP300 and CREBBP-mediated H3K27ac activation promotes SF3b4 transcription and expression in CRC. A. The UCSC Genome Bioinformatics website (http://genome.ucsc.edu/) showed high enrichment of H3K27ac in the SF3b4 promoter. B. Protein expression levels of SF3b4 and H3K27ac in HCT15 and HCT116 cells after treatment with C646 (20 μM) for 24 hours were detected by western blotting. C. Gene expression correlations among EP300, CREBBP, and SF3b4 were analyzed using GEPIA2 (http://gepia2.cancer-pku.cn/#index). D. Protein expression levels and efficiency of EP300, SF3b4, and H3K27ac in EP300-silenced HCT116 cells were detected by western blotting and RT-qPCR. E. Protein expression levels and efficiency of CREBBP, SF3b4, and H3K27ac in CREBBP-silenced HCT116 cells were detected by western blotting and RT-qPCR. F. In HCT116 cells with EP300 control or silencing, ChIP was used to detect EP300 binding levels on the SF3b4 promoter and H3K27ac enrichment in the SF3b4 promoter, respectively. G. In HCT116 cells with CREBBP control or silencing, ChIP was used to detect CREBBP binding levels on the SF3b4 promoter and H3K27ac enrichment in the SF3b4 promoter, respectively. H. Protein expression levels and efficiency of EP300, CREBBP, SF3b4, and H3K27ac in EP300- and CREBBP-co-silenced HCT116 cells were detected by western blotting. I. Schematic diagram of the mechanism by which EP300- and CREBBP-mediated H3K27ac activation induces SF3b4 transcription and translation. Data are presented as the mean ± standard deviation (SD) of three independent experiments. Compared with the control group, **P < 0.01, ***P < 0.001, ****P < 0.0001.

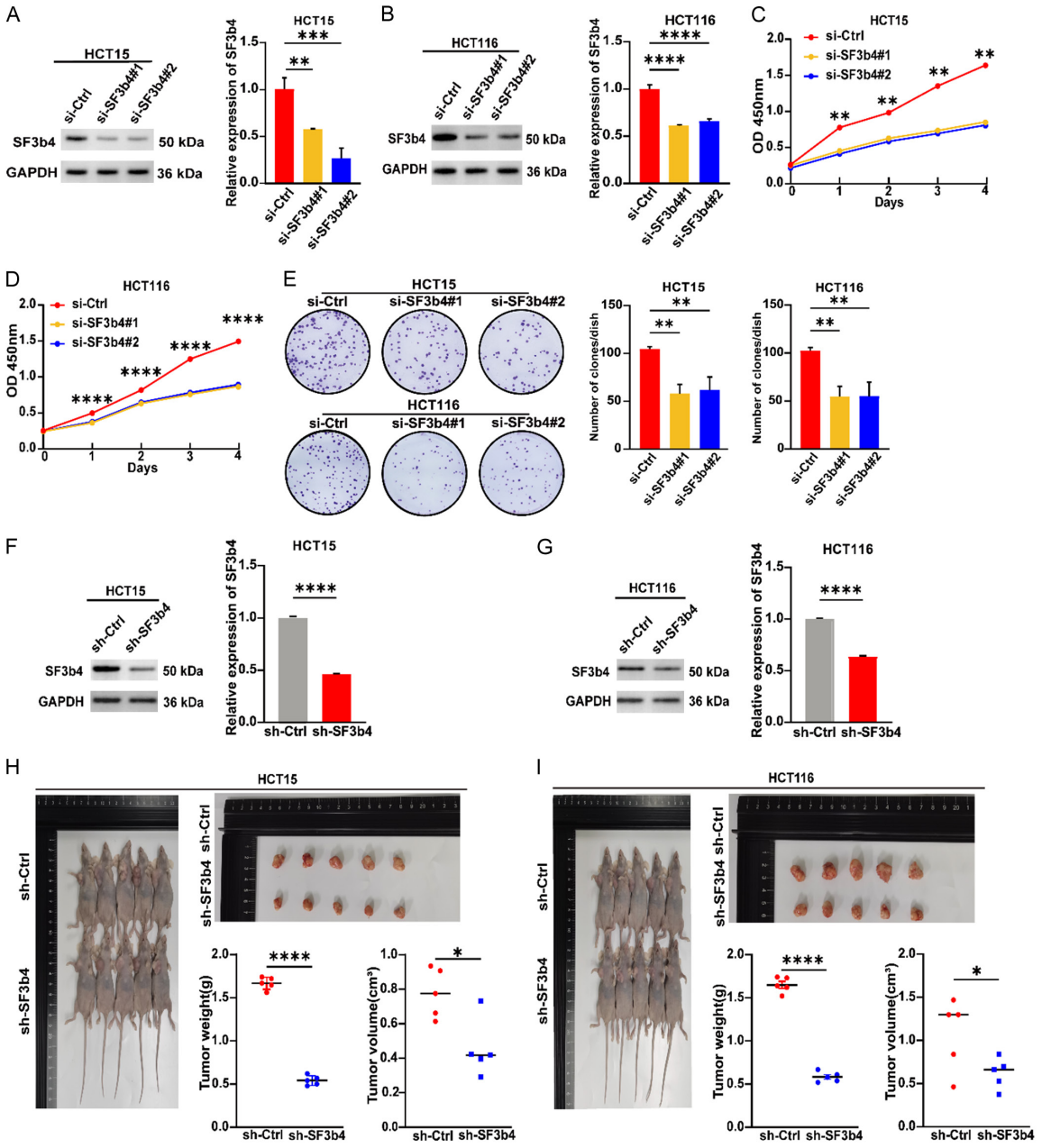

Figure 3. Effect of SF3b4 on colorectal cancer cell proliferation in vitro and in vivo. A. Protein and mRNA expression levels of SF3b4 in SF3b4-silenced HCT15 cells detected by western blotting and RT-qPCR. B. Protein and mRNA expression levels of SF3b4 in SF3b4-silenced HCT116 cells detected by western blotting and RT-qPCR. C, D. In vitro proliferation capacity of control and SF3b4-silenced HCT15 and HCT116 cells determined using the Cell Counting Kit-8 (CCK-8) and statistically analyzed. E. In vitro proliferation capacity of control and SF3b4-silenced HCT15 and HCT116 cells determined by colony formation assay and subjected to statistical analysis. F. Protein and mRNA expression levels of SF3b4 in stable SF3b4-knockdown HCT15 cells detected by western blotting and RT-qPCR. G. Protein and mRNA expression levels of SF3b4 in stable SF3b4-knockdown HCT116 cells detected by western blotting and RT-qPCR. H, I. Representative images of BALB/c nude mouse xenograft tumors in sh-Ctrl and sh-SF3b4 groups, along with corresponding excised tumors. Tumor weight and volume were measured and statistically analyzed. Data are presented as the mean ± standard deviation (SD) of three independent experiments. Compared with the control group, **P < 0.01, ***P < 0.001, ****P < 0.0001.

overexpression promoted CRC cell proliferation. sh-Ctrl+pcDNA3.1-ATG7 cells exhibited increased proliferation and colony-forming ability compared with sh-Ctrl, while sh-

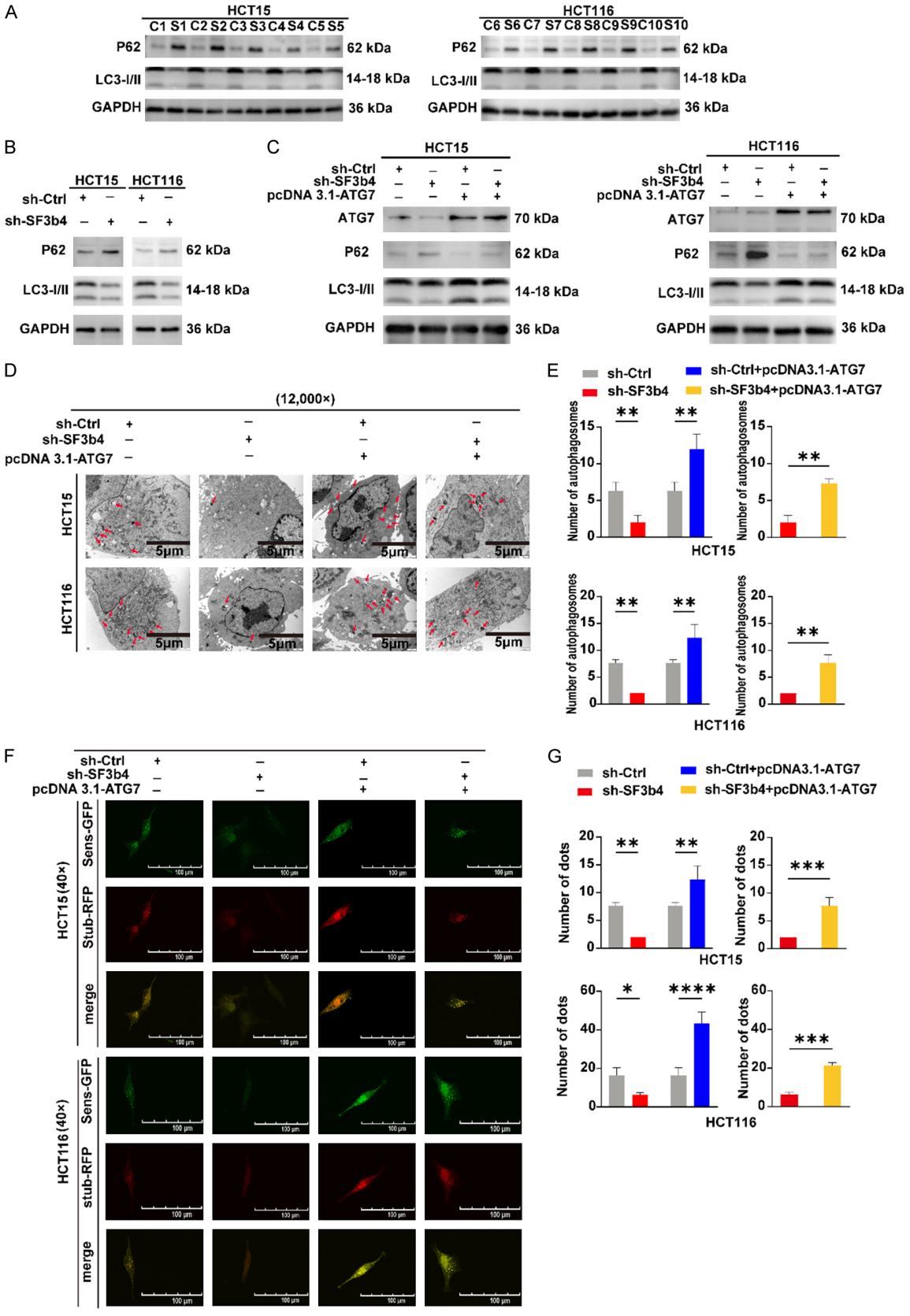

Figure 4. Effect of SF3b4 on autophagy in colorectal cancer. A. Expression of autophagic markers P62 and LC3I/II in xenograft tumors detected by western blotting, where C represents sh-Ctrl and S represents sh-SF3b4. B. Protein

expression levels of P62 and LC3I/II in SF3b4-knockdown HCT15 and HCT116 cells detected by western blotting. C. Protein expression levels of ATG7, P62, and LC3I/II in untransfected control (sh-Ctrl) and SF3b4-knockdown (sh-SF3b4) CRC cells, as well as control (sh-Ctrl+pcDNA3.1-ATG7) and SF3b4-knockdown (sh-SF3b4+pcDNA3.1-ATG7) CRC cells transfected with pcDNA3.1-ATG7 vector, detected by western blotting. D, E. Ultrastructural analysis (12,000× magnification) of autophagosome number changes in sh-Ctrl, sh-SF3b4, sh-Ctrl+pcDNA3.1-ATG7, and sh-SF3b4+pcDNA3.1-ATG7 CRC cells using transmission electron microscopy (TEM), with scale bar =5 μm and statistical analysis. F, G. Observation of autophagosome number changes labeled by stubRFP-sensGFP-LC3 lentivirus in sh-Ctrl, sh-SF3b4, sh-Ctrl+pcDNA3.1-ATG7, and sh-SF3b4+pcDNA3.1-ATG7 CRC cells under laser confocal microscopy (40× magnification), with scale bar =100 μm and statistical analysis. Data are presented as the mean ± standard deviation (SD) of three independent experiments. Compared with the control group, *P < 0.05, **P < 0.01, ***P < 0.001, ****P < 0.0001.

SF3b4+pcDNA3.1-ATG7 cells showed restored proliferation compared with sh-SF3b4 (**Figure 5A**, **5B**). Functional and pathway enrichment analyses of SF3b4-related genes from the TCGA CRC dataset (downloaded via cBioPortal and analyzed using WebGestalt) did not detect direct autophagy-related pathways among the top 20 enriched pathways (**Figure 5C**). However, cellular experiments suggest SF3b4 indirectly regulates autophagy via intermediate factors rather than direct involvement.

Collectively, these results demonstrate that autophagy enhancement via ATG7 overexpression promotes CRC cell proliferation and counteracts the proliferation-inhibiting effect of SF3b4 knockdown. SF3b4 likely indirectly modulates autophagy through intermediate factors and promotes tumor proliferation by enhancing autophagy in CRC cells.

Discussion

Current studies have found that, Elevated expression of SF3b4 has been implicated in the oncogenesis and progression of multiple malignant tumors, including hepatocellular carcinoma, ovarian cancer, cervical cancer, and non-small cell lung cancer. Bioinformatics analysis of public databases revealed that SF3b4 is significantly overexpressed in colorectal cancer (CRC) tissues compared to normal colorectal tissues. Consistent with database findings, SF3b4 expression levels were notably higher in CRC cell lines (SW480, SW620, LoVo, HCT15, and HCT116) than in the human normal colonic epithelial cell line FHC, providing a theoretical foundation for our study. Our results demonstrate that increased SF3b4 expression in CRC patients is correlated with lymph node metastasis, poor tumor differentiation, tumor size > 5 cm, and shorter postoperative survival duration. Previous studies have identified SF3b4 as an oncogene promoting malignant tumor proliferation and invasion across various cancer types [8-12, 27]. Collectively, these findings suggest that SF3b4 may contribute to CRC tumorigenesis and serve as a potential prognostic biomarker for the disease.

In this study, we demonstrated that SF3b4 promotes CRC cell proliferation both in vitro and in vivo. We further revealed that SF3b4 may enhance tumor cell autophagic activity indirectly through regulating certain intermediate factors to facilitate CRC progression. Due to the excessive growth of CRC, a unique tumor microenvironment characterized by hypoxia, low pH, and high metabolite levels is formed [28]. This environment renders tumor cells highly dependent on autophagy for energy supply [29-31]. Studies have shown that enhanced autophagy further promotes malignant tumor progression [32, 33], and recent research indicates that autophagy contributes to CRC cell proliferation [34], supporting our findings.

Knockdown of SF3b4 significantly reduced CRC cell proliferation, and these phenotypic changes induced by low SF3b4 expression were reversed by autophagy enhancement via ATG7 overexpression. Functional enrichment and pathway enrichment analyses showed no direct association with autophagic pathways among the top 20 significantly enriched pathways. However, our cellular experiments demonstrated that SF3b4 is involved in regulating autophagic activity in CRC cells. Therefore, we hypothesize that SF3b4 does not directly participate in autophagic regulation but indirectly influences autophagic mechanisms through modulating intermediate factors.

Collectively, these results suggest that SF3b4 promotes CRC proliferation and progression by indirectly enhancing autophagy through regulatory intermediate factors. Autophagy occurs in both normal and stressed tumor cells. This

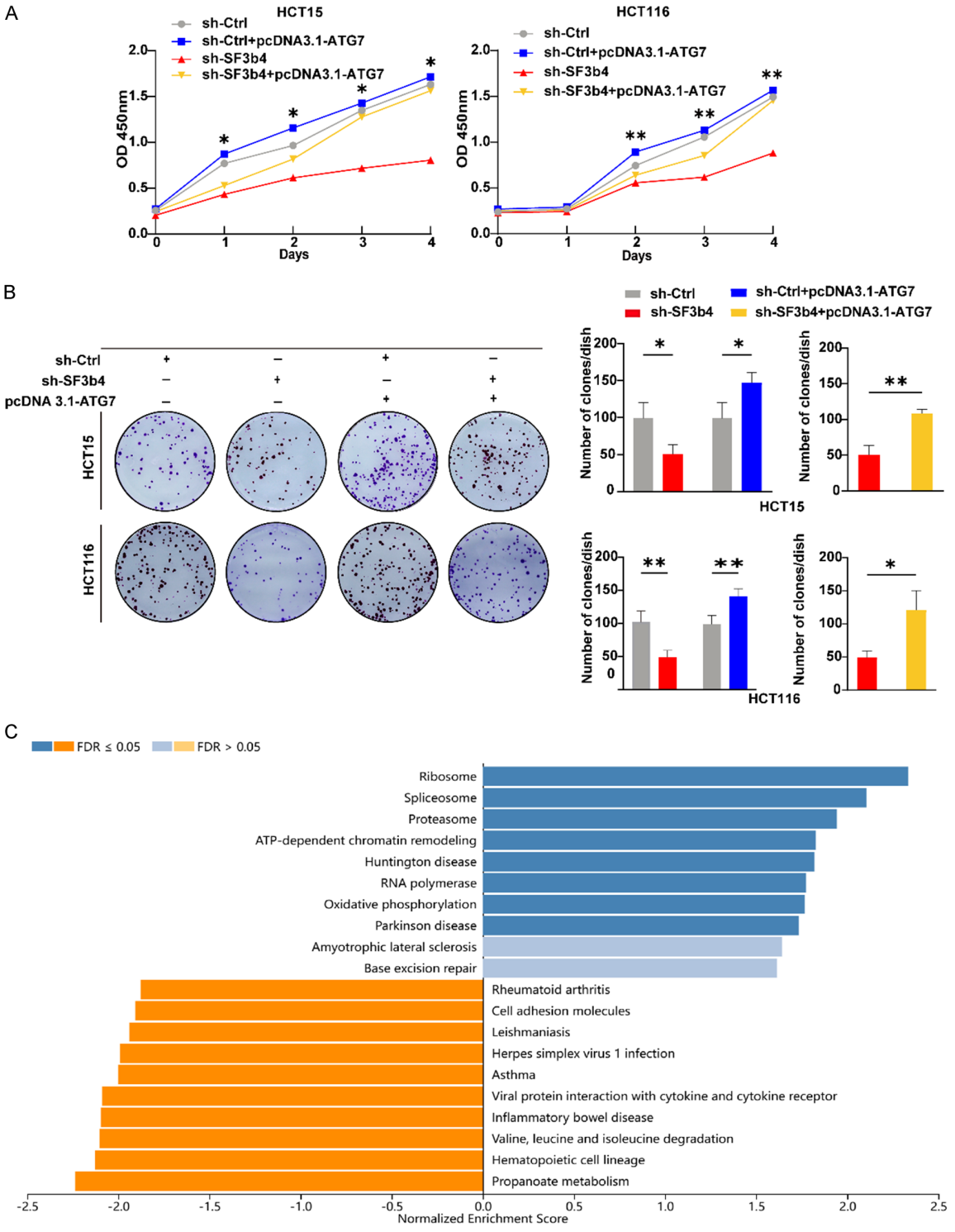

Figure 5. SF3b4 may indirectly influence autophagy through regulating certain intermediary factors, thereby affecting CRC cell proliferation. A. The proliferation capacity of CRC cells in sh-Ctrl, sh-SF3b4, sh-Ctrl+pcDNA3.1-ATG7, and sh-SF3b4+pcDNA3.1-ATG7 groups was validated using the Cell Counting Kit-8 (CCK-8). B. The proliferation capacity of CRC cells in the above groups was verified by colony formation assay and subjected to statistical analysis. C. Functional enrichment analysis and pathway enrichment analysis were performed using the cBioPortal database and WebGestalt tool. Data are presented as the mean ± standard deviation (SD) of three independent experiments. Compared with the control group, *P < 0.05, **P < 0.01.

study is the first to demonstrate that SF3b4 regulates autophagy in normal-state CRC cells and influences cell proliferation. However, the specific intermediate factors through which SF3b4 modulates autophagy in CRC, as well as its role in autophagy regulation under stress conditions (e.g., hypoxia, low pH, high metabolite levels), require further investigation.

While previous studies have shown that SF3b4 is negatively regulated by microRNA-133b (miR-133b) in hepatocellular carcinoma [8], negatively regulated by microRNA-509-3p (miR-509-3p) and positively regulated by SET domain bifurcated 1 (SETDB1) in ovarian cancer [9, 35], and upregulated by Methyltransferase-like 3 (METTL3)-mediated methylation in non-small cell lung cancer [10], the epigenetic regulation of SF3b4 in CRC remains unclear. To address this, we analyzed SF3b4 promoter modifications using the UCSC bioinformatics website and found significant enrichment of H3K27ac signals, indicating regulation by histone acetylation.

Given that H3K27ac is regulated by the EP300/CREBBP complex [36], we investigated whether EP300/CREBBP participates in SF3b4 regulation. Our results showed that EP300- and CREBBP-mediated H3K27ac acetylation activated the SF3b4 promoter and enhanced its transcriptional activity, leading to increased SF3b4 expression in CRC. CREBBP and EP300 are key acetyltransferases and transcriptional cofactors that regulate gene expression by modifying histone and non-histone acetylation levels [37]. Studies have confirmed that EP300 promotes tumorigenesis [38, 39], and EP300-mediated H3K27ac acetylation has been shown to activate promoters of several oncogenes, thereby enhancing their expression in tumors [25, 40]. Additionally, CREBBP is highly expressed in CRC and contributes to CRC development [41, 42], supporting our findings.

In summary, EP300/CREBBP-mediated H3K-27ac acetylation is a critical regulatory mechanism driving the oncogenic role of SF3b4 in CRC. However, further research is needed to clarify whether EP300 or CREBBP plays a dominant role in SF3b4 expression regulation.

Researchers have observed an intriguing phenomenon: SF3b4 is underexpressed and exerts a tumor suppressor role in pancreatic cancer and breast cancer [6, 12]. This discrepancy may be attributed to the tissue-specific functions of SF3b4 across different malignancies.

Collectively, our findings for the first time demonstrate that SF3b4 is highly expressed in CRC and possesses prognostic value in CRC patients. SF3b4 promotes CRC proliferation by indirectly regulating autophagic activity in CRC cells through certain intermediate factors. Mechanistically, we confirmed that EP300 and CREBBP regulate SF3b4 expression by activating H3K27ac acetylation on its promoter. These results indicate that SF3b4 acts as an oncogene in CRC and may serve as a potential prognostic biomarker for this disease.

Conclusions

In this study, we discovered that in colorectal cancer (CRC), H3K27ac acetylation on the SF3b4 promoter is activated by EP300 and CREBBP, thereby increasing SF3b4 expression levels. SF3b4 promotes CRC proliferation by indirectly enhancing cellular autophagy through certain intermediate factors. These results indicate that SF3b4 acts as an oncogene in CRC and may serve as a potential prognostic biomarker for CRC. This provides new insights into the mechanism underlying CRC development.

Ackonwledgements

The authors gratefully acknowledge the Scientific and Technological Innovation Center of North Sichuan Medical College and the Institute of Hepatobiliary, Pancreatic and Intestinal Diseases for providing essential research resources and technical support that significantly contributed to the completion of this study. The study was also supported by the National Clinical Key Specialty (General Surgery), Sichuan Provincial Clinical Key Specialty, the Sub-center of National Clinical Research Center for Digestive Diseases, and the Sichuan Clinical Research Center for Digestive Diseases. This research was funded by the Scientific Research Project of the Affiliated Hospital of North Sichuan Medical College (Grant No. 2022LC002).

Disclosure of conflict of interest

None.

Address correspondence to: Drs. Hongpeng Tian and Guangjun Zhang, Affiliated Hospital of North Sichuan Medical College, No. 1 Maoyuan South Road, Shunqing District, Nanchong 637000, Sichuan, China. E-mail: 1026176984@qq.com (HPT); zhanggj1977@126.com (GJZ)

References

[1] Bray F, Laversanne M, Sung H, Ferlay J, Siegel RL, Soerjomataram I and Jemal A. Global cancer statistics 2022: GLOBOCAN estimates of incidence and mortality worldwide for 36 cancers in 185 countries. CA Cancer J Clin 2024; 74: 229-263.

[2] Ma TF, Fan YR, Zhao YH and Liu B. Emerging role of autophagy in colorectal cancer: progress and prospects for clinical intervention. World J Gastrointest Oncol 2023; 15: 979-987.

[3] Golas MM, Sander B, Will CL, Luhrmann R and Stark H. Molecular architecture of the multiprotein splicing factor SF3b. Science 2003; 300: 980-984.

[4] Xiong F and Li S. SF3b4: a versatile player in eukaryotic cells. Front Cell Dev Biol 2020; 8: 14.

[5] Cassina M, Cerqua C, Rossi S, Salviati L, Martini A, Clementi M and Trevisson E. A synonymous splicing mutation in the SF3B4 gene segregates in a family with highly variable Nager syndrome. Eur J Hum Genet 2017; 25: 371-375.

[6] Denu RA and Burkard ME. Synchronous bilateral breast cancer in a patient with nager syndrome. Clin Breast Cancer 2017; 17: e151-e153.

[7] Petit F, Escande F, Jourdain AS, Porchet N, Amiel J, Doray B, Delrue MA, Flori E, Kim CA, Marlin S, Robertson SP, Manouvrier-Hanu S and Holder-Espinasse M. Nager syndrome: confirmation of SF3B4 haploinsufficiency as the major cause. Clin Genet 2014; 86: 246-251.

[8] Liu Z, Li W, Pang Y, Zhou Z, Liu S, Cheng K, Qin Q, Jia Y and Liu S. SF3B4 is regulated by microRNA-133b and promotes cell proliferation and metastasis in hepatocellular carcinoma. EBioMedicine 2018; 38: 57-68.

[9] Diao Y, Li Y, Wang Z, Wang S, Li P and Kong B. SF3B4 promotes ovarian cancer progression by regulating alternative splicing of RAD52. Cell Death Dis 2022; 13: 179.

[10] He G, Gu K, Wei J and Zhang J. METTL3-mediated the m6A modification of SF3B4 facilitates the development of non-small cell lung cancer by enhancing LSM4 expression. Thorac Cancer 2024; 15: 919-928.

[11] Yang Z, Wang YX, Wen JK, Gao HT, Han ZW, Qi JC, Gu JF, Zhao CM, Zhang H, Shi B, Wang DD, Wang XL and Qu CB. SF3B4 promotes Twist1 expression and clear cell renal cell carcinoma progression by facilitating the export of KLF 16 mRNA from the nucleus to the cytoplasm. Cell Death Dis 2023; 14: 26.

[12] Zhou W, Ma N, Jiang H, Rong Y, Deng Y, Feng Y, Zhu H, Kuang T, Lou W, Xie D and Wang D. SF3B4 is decreased in pancreatic cancer and inhibits the growth and migration of cancer cells. Tumour Biol 2017; 39: 1010428317695913.

[13] Ge S, Zhang Q and Yang X. GPAA1 promotes the proliferation, invasion and migration of hepatocellular carcinoma cells by binding to RNA-binding protein SF3B4. Oncol Lett 2022; 23: 160.

[14] Cheng Z. The foxo-autophagy axis in health and disease. Trends Endocrinol Metab 2019; 30: 658-671.

[15] Long J, He Q, Yin Y, Lei X, Li Z and Zhu W. The effect of miRNA and autophagy on colorectal cancer. Cell Prolif 2020; 53: e12900.

[16] Zhang S, Zhang J, An Y, Zeng X, Qin Z, Zhao Y, Xu H and Liu B. Multi-omics approaches identify SF3B3 and SIRT3 as candidate autophagic regulators and druggable targets in invasive breast carcinoma. Acta Pharm Sin B 2021; 11: 1227-1245.

[17] Shen Q and Nam SW. SF3B4 as an early-stage diagnostic marker and driver of hepatocellular carcinoma. BMB Rep 2018; 51: 57-58.

[18] Shen Q, Eun JW, Lee K, Kim HS, Yang HD, Kim SY, Lee EK, Kim T, Kang K, Kim S, Min DH, Oh SN, Lee YJ, Moon H, Ro SW, Park WS, Lee JY and Nam SW. Barrier to autointegration factor 1, procollagen-lysine, 2-oxoglutarate 5-dioxygenase 3, and splicing factor 3b subunit 4 as early-stage cancer decision markers and drivers of hepatocellular carcinoma. Hepatology 2018; 67: 1360-1377.

[19] Slusher AL, Kim JJ, Ribick M, Pollens-Voigt J, Bankhead A, Palmbos PL and Ludlow AT. Intronic cis-element DR8 in hTERT is bound by splicing factor SF3B4 and regulates hTERT splicing in non-small cell lung cancer. Mol Cancer Res 2022; 20: 1574-1588.

[20] Chandrashekar DS, Bashel B, Balasubramanya SAH, Creighton CJ, Ponce-Rodriguez I, Chakravarthi BVSK and Varambally S. UALCAN: a portal for facilitating tumor subgroup gene expression and survival analyses. Neoplasia 2017; 19: 649-658.

[21] Chandrashekar DS, Karthikeyan SK, Korla PK, Patel H, Shovon AR, Athar M, Netto GJ, Qin ZS, Kumar S, Manne U, Creighton CJ and Varambally S. UALCAN: an update to the integrated cancer data analysis platform. Neoplasia 2022; 25: 18-27.

[22] Gyorffy B. Integrated analysis of public datasets for the discovery and validation of survival-

associated genes in solid tumors. Innovation (Camb) 2024; 5: 100625.
[23] Gyorffy B. Transcriptome-level discovery of survival-associated biomarkers and therapy targets in non-small-cell lung cancer. Br J Pharmacol 2024; 181: 362-374.
[24] Nassar LR, Barber GP, Benet-Pages A, Casper J, Clawson H, Diekhans M, Fischer C, Gonzalez JN, Hinrichs AS, Lee BT, Lee CM, Muthuraman P, Nguy B, Pereira T, Nejad P, Perez G, Raney BJ, Schmelter D, Speir ML, Wick BD, Zweig AS, Haussler D, Kuhn RM, Haeussler M and Kent WJ. The UCSC Genome Browser database: 2023 update. Nucleic Acids Res 2023; 51: D1188-D1195.
[25] Wang Q, Chen C, Ding Q, Zhao Y, Wang Z, Chen J, Jiang Z, Zhang Y, Xu G, Zhang J, Zhou J, Sun B, Zou X and Wang S. METTL3-mediated m(6)A modification of HDGF mRNA promotes gastric cancer progression and has prognostic significance. Gut 2020; 69: 1193-1205.
[26] Collier JJ, Suomi F, Olahova M, McWilliams TG and Taylor RW. Emerging roles of ATG7 in human health and disease. EMBO Mol Med 2021; 13: e14824.
[27] Li Y, Diao Y, Wang Z, Wang S, Peng J and Kong B. The splicing factor SF3B4 drives proliferation and invasion in cervical cancer by regulating SPAG5. Cell Death Discov 2022; 8: 326.
[28] Hinshaw DC and Shevde LA. The tumor microenvironment innately modulates cancer progression. Cancer Res 2019; 79: 4557-4566.
[29] Ganapathy-Kanniappan S and Geschwind JF. Tumor glycolysis as a target for cancer therapy: progress and prospects. Mol Cancer 2013; 12: 152.
[30] Paul S, Ghosh S and Kumar S. Tumor glycolysis, an essential sweet tooth of tumor cells. Semin Cancer Biol 2022; 86: 1216-1230.
[31] Li CH and Liao CC. The metabolism reprogramming of microRNA let-7-mediated glycolysis contributes to autophagy and tumor progression. Int J Mol Sci 2021; 23: 113.
[32] Bai Y, Liu X, Qi X, Liu X, Peng F, Li H, Fu H, Pei S, Chen L, Chi X, Zhang L, Zhu X, Song Y, Wang Y, Meng S, Jiang T and Shao S. PDIA6 modulates apoptosis and autophagy of non-small cell lung cancer cells via the MAP4K1/JNK signaling pathway. EBioMedicine 2019; 42: 311-325.
[33] Liang G, Ling Y, Mehrpour M, Saw PE, Liu Z, Tan W, Tian Z, Zhong W, Lin W, Luo Q, Lin Q, Li Q, Zhou Y, Hamai A, Codogno P, Li J, Song E and Gong C. Autophagy-associated circRNA circCDYL augments autophagy and promotes breast cancer progression. Mol Cancer 2020; 19: 65.
[34] Li Q, Wang Z, Wang J, Wang J, Zheng X, Li D, Wang Z, Li J and Li Y. Regulatory feedback loop between circ-EIF4A3 and EIF4A3 Enhances autophagy and growth in colorectal cancer cells. Transl Oncol 2024; 46: 101996.
[35] Yang H, Sui L, Cai C, Chu H and Diao Y. SETDB1 promotes progression through upregulation of SF3B4 expression and regulates the immunity in ovarian cancer. J Ovarian Res 2024; 17: 34.
[36] Ding H, Pei Y, Li Y, Xu W, Mei L, Hou Z, Guang Y, Cao L, Li P, Cao H, Bian J, Chen K, Luo C, Zhou B, Zhang T, Li Z and Yang Y. Design, synthesis and biological evaluation of a novel spiro oxazolidinedione as potent p300/CBP HAT inhibitor for the treatment of ovarian cancer. Bioorg Med Chem 2021; 52: 116512.
[37] Hennig AK, Peng GH and Chen S. Transcription coactivators p300 and CBP are necessary for photoreceptor-specific chromatin organization and gene expression. PLoS One 2013; 8: e69721.
[38] Iyer NG, Ozdag H and Caldas C. p300/CBP and cancer. Oncogene 2004; 23: 4225-4231.
[39] Yan G, Eller MS, Elm C, Larocca CA, Ryu B, Panova IP, Dancy BM, Bowers EM, Meyers D, Lareau L, Cole PA, Taverna SD and Alani RM. Selective inhibition of p300 HAT blocks cell cycle progression, induces cellular senescence, and inhibits the DNA damage response in melanoma cells. J Invest Dermatol 2013; 133: 2444-2452.
[40] Liu J. P300 increases CSNK2A1 expression which accelerates colorectal cancer progression through activation of the PI3K-AKT-mTOR axis. Exp Cell Res 2023; 430: 113694.
[41] Bordonaro M and Lazarova DL. CREB-binding protein, p300, butyrate, and Wnt signaling in colorectal cancer. World J Gastroenterol 2015; 21: 8238.
[42] Chung DJ, Wang CH, Liu PJ, Ng SK, Luo CK, Jwo SH, Li CT, Hsu DY, Fan CC and Wei TT. Targeting CREB-binding protein (CBP) abrogates colorectal cancer stemness through epigenetic regulation of C-MYC. Cancer Gene Ther 2024; 31: 1734-1748.